Article

Cell Reports

Comprehensive Analysis of a *cis*-Regulatory Region Reveals Pleiotropy in Enhancer Function

Graphical Abstract

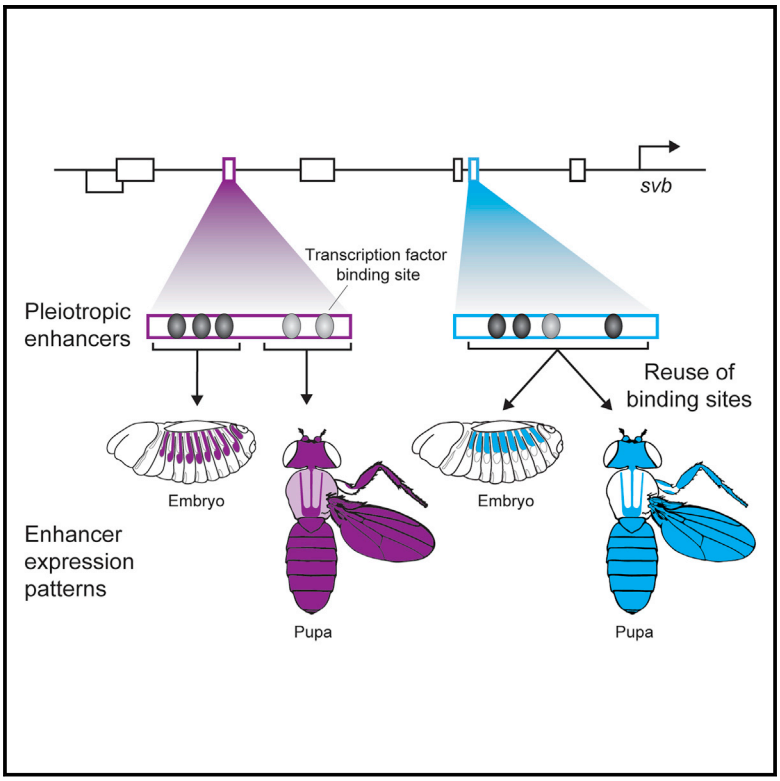

Authors

Ella Preger-Ben Noon, Gonzalo Sabarís, Daniela M. Ortiz, Jonathan Sager, Anna Liebowitz, David L. Stern, Nicolás Frankel

Correspondence

sternd@janelia.hhmi.org (D.L.S.), nfrankel@ege.fcen.uba.ar (N.F.)

In Brief

Preger-Ben Noon et al. find that *shavenbaby* gene enhancers contain regulatory information for driving several expression patterns (i.e., enhancers are pleiotropic) and that, in some cases, the transcription factor binding sites that activate these enhancers are reused during development.

Highlights

- Pleiotropic enhancers drive the various expression patterns of the *shavenbaby* gene
- Transcription factor binding sites can be reused at different developmental stages
- Pleiotropic enhancers drive gene expression at varying levels of redundancy
- Extensive redundancy in the pupal stage might release constraints on enhancer evolution

Preger-Ben Noon et al., 2018, Cell Reports *22*, 3021–3031
March 13, 2018
https://doi.org/10.1016/j.celrep.2018.02.073

CellPress

Cell Reports
Article

Comprehensive Analysis of a *cis*-Regulatory Region Reveals Pleiotropy in Enhancer Function

Ella Preger-Ben Noon,[1,4] Gonzalo Sabarís,[2,4] Daniela M. Ortiz,[2] Jonathan Sager,[1] Anna Liebowitz,[3] David L. Stern,[1,*] and Nicolás Frankel[2,5,*]

[1]Howard Hughes Medical Institute (HHMI), Janelia Research Campus, Ashburn, VA 20147, USA
[2]Departamento de Ecología, Genética y Evolución, IEGEBA-CONICET, Facultad de Ciencias Exactas y Naturales, Universidad de Buenos Aires, Buenos Aires 1428, Argentina
[3]Department of Molecular Biology, Princeton University, Princeton, NJ 08544, USA
[4]These authors contributed equally
[5]Lead Contact
*Correspondence: sternd@janelia.hhmi.org (D.L.S.), nfrankel@ege.fcen.uba.ar (N.F.)
https://doi.org/10.1016/j.celrep.2018.02.073

SUMMARY

Developmental genes can have complex *cis*-regulatory regions with multiple enhancers. Early work revealed remarkable modularity of enhancers, whereby distinct DNA regions drive gene expression in defined spatiotemporal domains. Nevertheless, a few reports have shown that enhancers function in multiple developmental stages, implying that enhancers can be pleiotropic. Here, we have studied the activity of the enhancers of the *shavenbaby* gene throughout *D. melanogaster* development. We found that all seven *shavenbaby* enhancers drive expression in multiple tissues and developmental stages. We explored how enhancer pleiotropy is encoded in two of these enhancers. In one enhancer, the same transcription factor binding sites contribute to embryonic and pupal expression, revealing site pleiotropy, whereas for a second enhancer, these roles are encoded by distinct sites. Enhancer pleiotropy may be a common feature of *cis*-regulatory regions of developmental genes, and site pleiotropy may constrain enhancer evolution in some cases.

INTRODUCTION

Developmental genes can have complex *cis*-regulatory regions, with multiple enhancers scattered across stretches of DNA spanning tens or hundreds of kilobases (Kim et al., 2013; Zeitlinger et al., 2007; Williamson et al., 2016; Montavon et al., 2011). Over many years, numerous studies have revealed remarkable modularity of enhancer function, whereby distinct regions of DNA, bound by combinations of transcription factors, drive gene expression in defined spatiotemporal domains (Davidson, 2010). It has long been hypothesized that enhancer modularity facilitates evolution, because mutations in one enhancer can alter gene function without affecting the activity of other enhancers, thereby minimizing pleiotropic effects (Stern, 2000; Carroll, 2008; Wittkopp and Kalay, 2011). It is not clear, however, if the apparent modularity of enhancers reflects ascertainment bias, as few studies have looked explicitly for pleiotropy.

Pleiotropy occurs when a single genetic element functions in more than one spatiotemporal context. Many genes that regulate development have a role in multiple tissues and/or their function is required at various developmental stages, a characteristic that has been termed "gene pleiotropy" (Paaby and Rockman, 2013). A second level of pleiotropy, named "enhancer pleiotropy" (Monteiro and Podlaha, 2009), occurs when small DNA regions (i.e., pleiotropic enhancers), contain the regulatory information and provide the proper epigenetic landscape for driving more than one expression pattern. For example, single enhancers of *Hox* genes drive expression in both digits and genitalia of the mouse (Lonfat et al., 2014), and these enhancers are decorated with similar epigenetic marks in both organs (Lonfat et al., 2014). It is not clear, however, whether pleiotropic enhancers use the same transcription factor binding sites to drive expression in multiple contexts or whether enhancers function as chromatin scaffolds, whereby independent sets of binding sites are used to drive different expression patterns. If transcription factor binding sites were to be reused in more than one context, it could be said that there is "site pleiotropy."

shavenbaby (*svb*) encodes a transcription factor that orchestrates the differentiation of non-sensory cuticular projections (hereafter called trichomes) in *Drosophila melanogaster* (Stern and Frankel, 2013; Arif et al., 2015). *Svb* expression has been studied in detail mainly in the late embryonic stages, when it directs development of the epidermis and, concomitantly, the first-instar larval cuticle (Payre et al., 1999). *Svb* is also expressed in the pupal epidermis, where it is required for trichome development in part of the wing, notum, and abdomen (Delon et al., 2003; Chanut-Delalande et al., 2014) and for proper development of leg joints (Pueyo and Couso, 2011).

The *cis*-regulatory region of the *svb* gene has been experimentally dissected in *D. melanogaster* (Preger-Ben Noon et al., 2016; Crocker et al., 2015; Frankel et al., 2010, 2011; McGregor et al., 2007). The embryonic expression of *svb* is generated by seven enhancers that are located in a ~80 kb region upstream of the

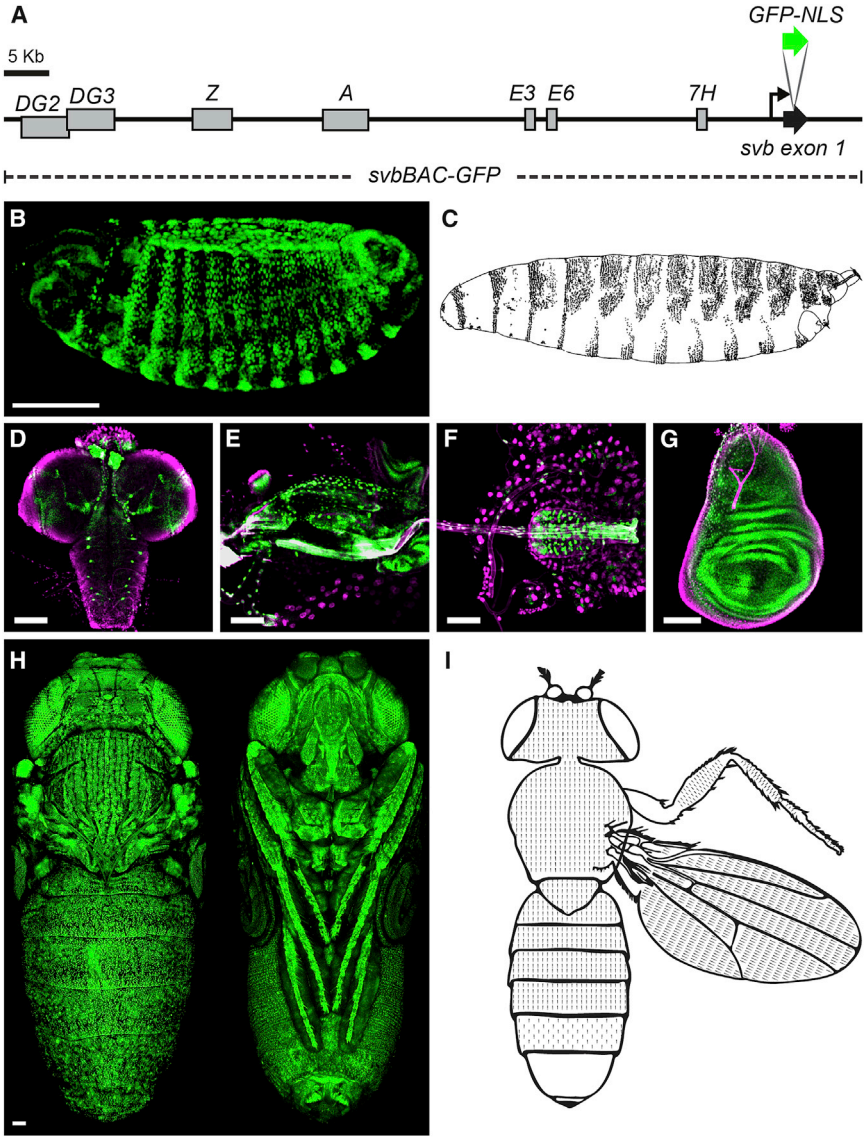

Figure 1. *svb* Expression throughout *Drosophila melanogaster* Development

(A) Schematic representation of *svb*BAC-GFP. Gray boxes represent the seven embryonic enhancers. The site of insertion of the GFP-NLS is indicated in the scheme.

(B) GFP expression recapitulates the expression pattern of *svb* in the embryo.

(C) Trichome pattern of the first-instar larva.

(D–G) GFP expression in non-epidermal structures of the third-instar larva: CNS (D), pharynx and salivary glands (E), esophagus and proventriculus (F), and wing imaginal disc (G). DAPI stain in magenta.

(H) GFP expression in pupal epidermis.

(I) Representation of the trichome pattern in the dorsum of an adult fly.

The scale bars represent 100 μm.

transcription start site of the gene (Stern and Frankel, 2013; Figure 1A). These seven enhancers drive partially overlapping expression patterns in the late embryo that are required for robust gene expression (Frankel et al., 2010). Evolutionary changes in five of these enhancers led to reduced *svb* expression in the dorsum of the *D. sechellia* embryo, resulting in differentiation of naked cuticle, rather than trichomes, in the first-instar larva of *D. sechellia* (Stern and Frankel, 2013; Frankel et al., 2010; Frankel et al., 2011; McGregor et al., 2007).

In this work, we show that *svb* is a pleiotropic gene and that all seven *svb* enhancers are pleiotropic enhancers that drive gene expression at varying levels of redundancy. We have explored how pleiotropy is encoded in two of these enhancers. In one enhancer, the same transcription factor binding sites contribute to embryonic and pupal expression, revealing site pleiotropy, whereas for a second enhancer these roles are encoded by distinct sites.

RESULTS

shavenbaby Is a Pleiotropic Gene

We first sought to characterize *svb* expression in larval and pupal tissues. To that end, we engineered a BAC carrying the complete *cis*-regulatory region of *svb* by placing the coding sequence of a nuclear GFP downstream of the *svb* ATG (Figure 1A). We stably integrated this BAC, named *svb*BAC-GFP, in the fly genome through attP/attB recombination. We confirmed that *svb*BAC-GFP recapitulates the expression of the native gene in embryos (Figures 1B and S1). This epidermal expression prefigures the location of trichomes in the first-instar larva cuticle (Figure 1C). We then examined *svb* expression in later stages. We observed GFP expression in the epidermis of third-instar larvae (data not shown). This may reflect persistence of the GFP reporter from second-instar larvae, when *svb* expression is probably required to cause differentiation of trichomes that will decorate the cuticle of third-instar larvae. We also detected GFP expression in larval non-epidermal structures of ectodermal origin that do not produce trichomes. Specifically, we observed GFP in the CNS (Figure 1D), the foregut (Figures 1E and 1F), the wing imaginal discs (Figure 1G), the haltere, leg, and eye-antennal discs (data not shown), and the trachea (data not shown). We also found that *svb*BAC-GFP displayed GFP expression in all pupal epidermal tissues (Figure 1H), which is consistent with the fact that the adult exoskeleton is almost completely covered with trichomes (Figure 1I).

shavenbaby Is Required for the Formation of Many, but Not All, Adult Trichomes

Next we asked whether *svb* function is required for trichome development in the pupal epidermis, as it is in the embryo

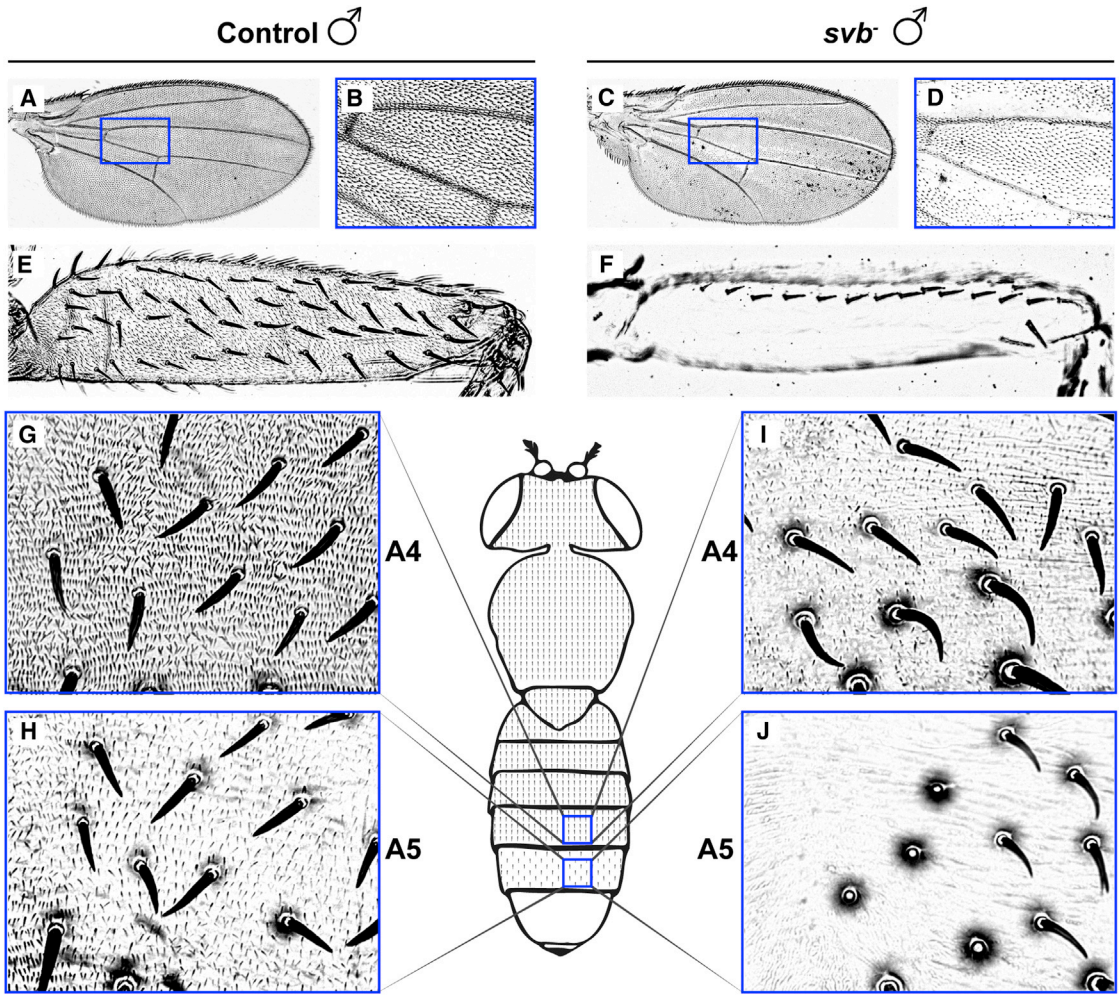

Figure 2. *svb* Is Required for the Production of Trichomes in the Adult Cuticle

(A–J) The cuticle of control f[36a] adult wing (A and B), leg (E), and abdomen (G and H) is covered with trichomes. In *svb*-null male escapers (f[36a], svb^1/Y; C, D, F, I, and J) many trichomes, but not all, are replaced by naked cuticle. A complete loss of trichomes is observed in legs (F) and abdominal segment A5 (J). Blue boxes within the cartoon demarcate the imaged area.

(Payre et al., 1999). Flies carrying *svb*-null mutations normally die before they eclose, but we identified a few male escapers (carrying a null *svb* allele on their single X chromosome) that allowed us to assess the requirement of *svb* for trichome development in the adult cuticle. Escapers had fewer trichomes in the wing, the legs, and the dorsal abdomen than control flies, but they still retained trichomes over much of the exoskeleton (Figure 2). However, in most regions, trichomes were smaller than normal or were misshapen.

We observed that no trichomes developed in male *svb* escapers on the dorsal abdominal segment 5 (compare Figures 2H and 2J). This observation stimulated a detailed inspection of the wild-type trichome pattern, and we found a sexual dimorphism in the shape and size of trichomes in the dorsal abdomen: females produce trichomes of similar density and stoutness on abdominal segments A1 through A5 (Figure S1C), whereas males produce qualitatively different trichomes on abdominal segments A1–A4 versus A5 (Figure S1C). We observed that *svb* expression is lower in abdominal segment 5 versus more anterior segments in both sexes and this difference may contribute to the sexual dimorphism in trichome patterning (Figure S1D). It is intriguing that although *svb* is expressed in A6 (Figure 1H), no trichomes are formed in this segment. It is possible that *svb* expression is not sufficient to activate trichome formation or that trichome development is suppressed by another mechanism.

We confirmed the results observed with the male escapers by generating *svb*−/− clones in the adult. We observed loss of trichomes in *svb*−/− clones in the same regions where trichomes were lost in male escapers (see Figure S2A for an example), confirming that *svb* function is required for the production of some adult trichomes. We also observed loss of trichomes, change in trichome morphology, and altered trichome distribution in the head cuticle (Figure S2B). Loss of *svb* function also modified the anatomy of the antennal arista (Figures S2C and S2D). In summary, although *svb* is expressed throughout the pupal

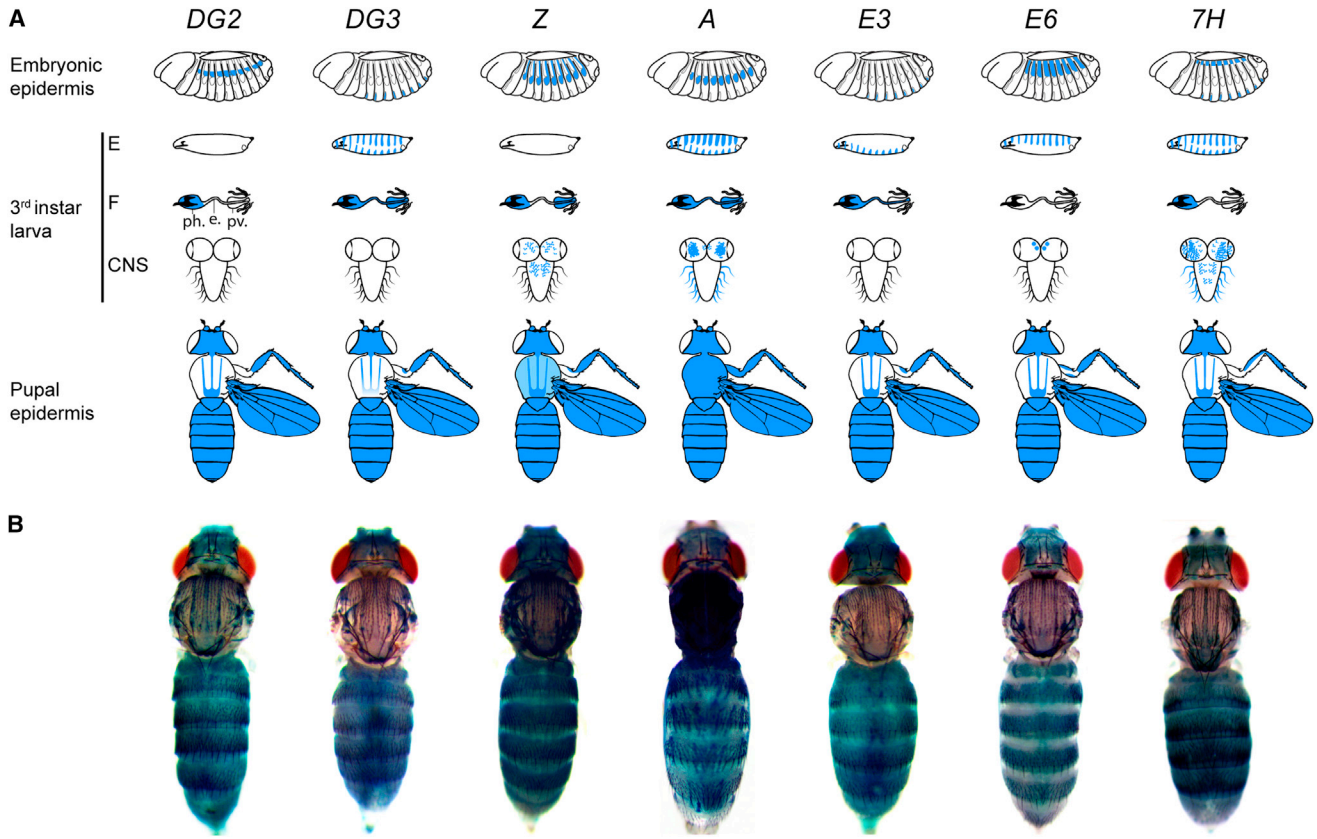

Figure 3. Pleiotropy and Redundancy in the Activity of the Seven *svb* Embryonic Enhancers

(A) Schematization of the expression pattern driven by each enhancer (blue) in embryo (top), third-instar larva (middle), and pupa (bottom) (see Figure S3 for details). E, epidermis; e, esophagus; F, foregut; ph, pharynx; pv, proventriculus.

(B) Expression pattern generated by each enhancer in the dorsal epidermis of the head, thorax, and abdomen (90 hr APF).

epidermis (Figure 1H), it is required for the normal development of many, but not all, adult trichomes.

The Embryonic Enhancers of *shavenbaby* Are Pleiotropic

Considering that *svb* is a pleiotropic gene, we wondered whether this gene contains pleiotropic enhancers. Because the BAC containing the complete *svb* regulatory region drives expression in embryonic, larval, and pupal stages, we analyzed whether the previously characterized embryonic enhancers also drove expression in later stages. In the third-instar larvae, we found that of the seven embryonic *svb* enhancers, five drove expression in the epidermis, six drove expression in the foregut, and four drove expression in the CNS (Figures 3A and Figure S3A). These results are consistent with the expression of the *svb*BAC-GFP (Figure 1). In the pupa at 90 hr after puparium formation (APF), all embryonic *svb* enhancers drove widespread epidermal expression (Figures 3A, 3B, and S3B). Most notably, all seven enhancers drove expression throughout the dorsal abdomen (Figure 3B). This level of overlapping expression far exceeds the pattern of overlapping embryonic expression that we reported previously (Frankel et al., 2010). Hence, we decided to explore the function of this redundancy within the whole *cis*-regulatory region of *svb*.

Deletion of Individual Enhancers Has Contrasting Outcomes in Embryo and Pupa

In recent years it has become evident that the expression of many developmental genes is controlled by multiple enhancers with redundant functions (Frankel, 2012). We have previously demonstrated that *svb* enhancers drive partially redundant expression patterns in the embryo (Figure 3A), providing phenotypic robustness for larval trichome patterns in the face of environmental and genetic variation (Frankel et al., 2010). Given the remarkable redundancy of *svb* enhancer function observed in pupae (Figure 3B), we hypothesized that robustness of *svb* expression during pupal development is even greater than during embryogenesis. We therefore tested how removal of individual enhancers affects gene expression at these two developmental stages.

We targeted three enhancers positioned at varying distance from the basal promoter (*Z*, *E6*, and *7H*). In order to remove fragments of similar sizes in all cases, and considering that *E6* and *7H* encompass ~1 kb, we dissected the 4.4 kb of *Z* to a 1.3 kb region that retained similar expression to the full *Z* region, named *Z1.3* (see Figure S4 for details). We used BAC recombineering to delete individual enhancers in the *svb*BAC-GFP and integrated these BACs in a specific *attP* site of the *D. melanogaster* genome

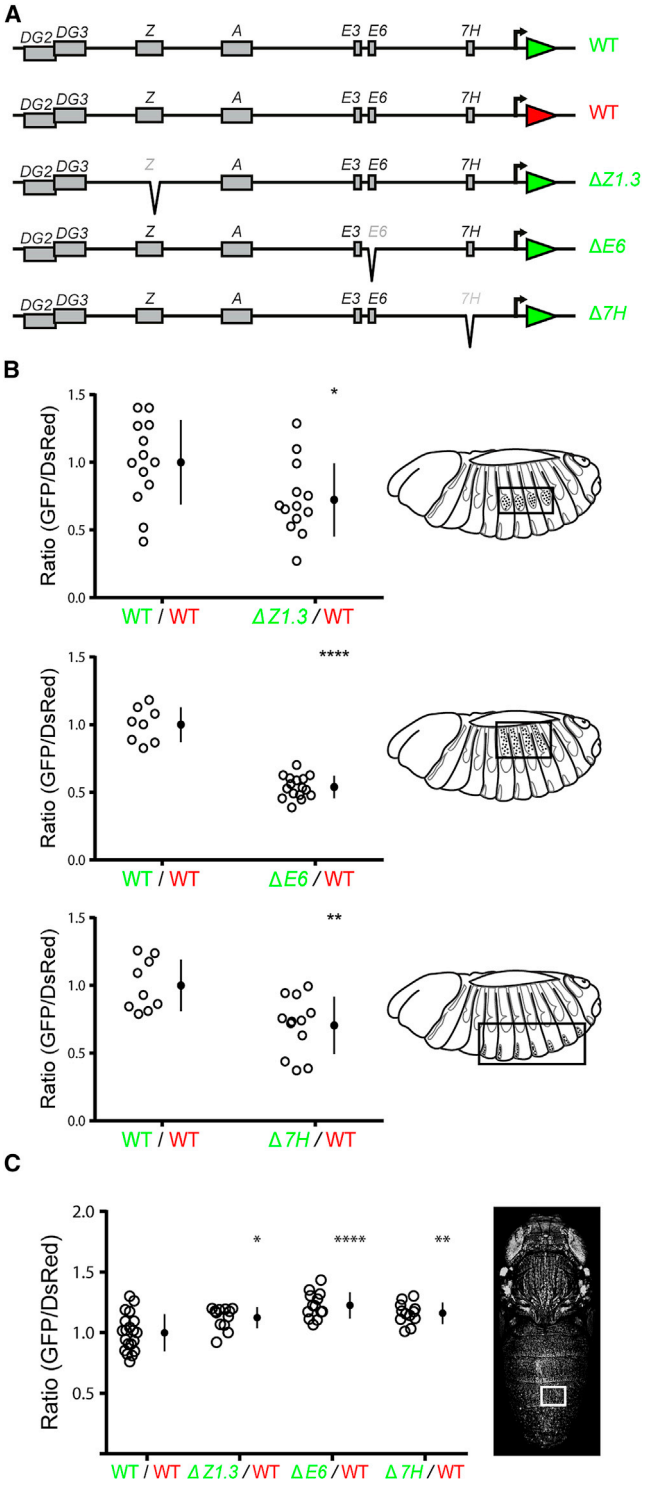

Figure 4. *cis*-Regulation of *svb* Varies between Embryo and Pupa

(A) Wild-type and mutated versions of the *svb*BAC. The green and red triangles depict the coding sequence of GFP and DsRed, respectively.

(B) Effect of enhancer deletions in embryonic expression: Δ*Z1.3* (top), Δ*E6* (middle), and Δ*7H* (bottom). Open circles indicate the average ratio (GFP/DsRed) for each individual. Closed black circles and vertical lines indicate mean and 1 SD, respectively. p values were calculated using two-tailed unpaired t tests (*$p < 0.05$, **$p < 0.005$, and ****$p < 0.0001$). Boxes within embryo cartoons specify analyzed regions.

(C) Effect of enhancer deletions on pupal expression. The GFP/DsRed ratio was measured in part of abdominal segment A4 (rectangle) of pupae 90 hr APF. Open circles indicate the average ratio (GFP/DsRed) for each individual. Closed black circles and vertical lines indicate mean and 1 SD, respectively. Statistical significance was calculated using one-way ANOVA and Dunnett's pairwise comparisons (*$p < 0.05$, **$p < 0.005$, and ****$p < 0.0001$).

(Figure 4A). As an internal control we used a wild-type *svb*BAC with a DsRed reporter (*svb*BAC-DsRed) that was integrated into a different *attP* site (to avoid transvection effects between BACs). We then quantified expression patterns of the BACs carrying deletions (expressing GFP) relative to the control BAC (expressing DsRed) in the same animal (Figures 4 and S5; see Experimental Procedures for details).

Removing *Z1.3*, *E6*, or *7H* resulted in a decrease of the mean GFP expression in embryos of 28%, 46%, and 38%, respectively (Figure 4B). However, none of the BACs with enhancer deletions drove reduced reporter expression in the pupal epidermis of abdominal segment A4 (Figure 4C). On the contrary, deletion of single enhancers slightly increased reporter expression (12%, 23%, and 16% for *Z1.3*, *E6*, and *7H*, respectively). These results suggest that the function of individual enhancers within the whole *cis*-regulatory region of *svb* changes during development.

Deletion of Multiple Enhancers in the *shavenbaby* Locus Does Not Affect the Adult Trichome Pattern

To examine the importance of enhancer redundancy on the phenotypic output of *svb* function, we examined the effects of deficiencies that remove part of the *svb* regulatory region in the native locus. We used *Df(X)svb*^{108}, a deletion of the three most distal enhancers (*DG2*, *DG3*, and *Z*; Frankel et al., 2010) and a newly generated larger deletion, *Df(X)svb*^{106}, that removes the four most distal enhancers (*DG2*, *DG3*, *Z*, and *A*; Figure 5A). We have previously shown that the *Df(X)svb*^{108} line produces a normal number of first-instar larval trichomes when embryos develop at their optimal temperature of 25°C (Frankel et al., 2010). However, when embryos are grown at a stressful temperature, 32°C, they develop with significantly fewer larval trichomes (Frankel et al., 2010). We found that *Df(X)svb*^{106} produced similar results (data not shown).

We could not find any gross changes in the trichome pattern of females (data not shown) when pupae were grown at 25°C. We did notice, however, a small but consistent trichome defect in males carrying either deficiency grown at 25°C: the dorsum of abdominal segment A5 had fewer trichomes than in wild-type males (Figure 5B). This result is consistent with the phenotype of male *svb* escapers (Figure 2J) and the observation that *svb* is expressed in this abdominal segments at lower levels (Figure S1D). Growing *Df(X)svb*^{108} or *Df(X)svb*^{106} pupae at 32°C gave the same results that were obtained with 25°C (data not shown). Hence, the adult trichome pattern is largely robust to removal of up to four of the seven *svb* enhancers. In contrast to the effect of these deficiencies on first-instar larvae, stressful growth temperatures in pupa did not significantly alter adult trichome development. We hypothesize that this extreme

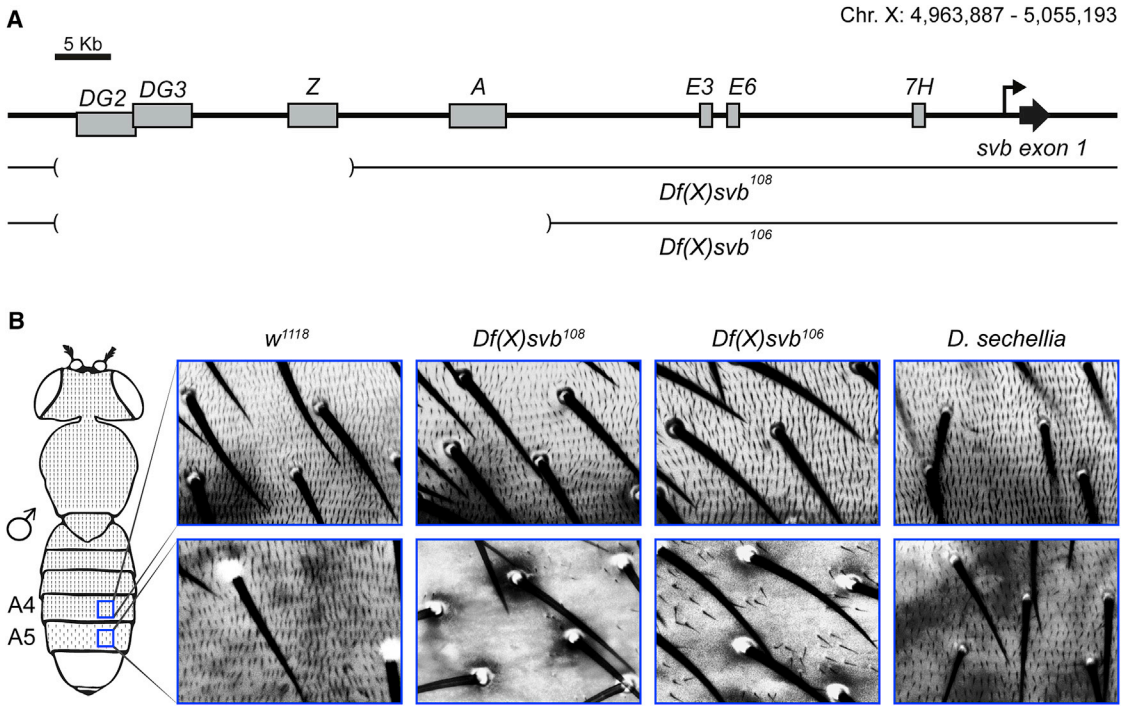

Figure 5. Enhancer Deletions in the Native *svb* Locus Alter the A5 Trichome Pattern Only in Males

(A) Diagram of the *svb* locus showing the genomic deletions on the X chromosome of lines *Df(X)svb*^{108} and *Df(X)svb*^{106}. Deletion in *Df(X)svb*^{108} removes enhancers *DG2*, *DG3*, and *Z*, while *Df(X)svb*^{106} deletion removes enhancers *DG2*, *DG3*, *Z*, and *A*.

(B) A4 and A5 trichome pattern in adult males of *D. melanogaster*, *Df(X)svb*^{108}, *Df(X)svb*^{106}, and *D. sechellia*. Blue boxes within the cartoon demarcate the imaged area.

robustness in adult trichome pattern results from the fact that most *svb* enhancers drive expression in epidermal tissues that produce adult trichomes.

Understanding How Pleiotropy Is Encoded within Enhancers

We next sought to understand the mechanism through which a single enhancer can encode multiple expression patterns. As an entry point to this problem we exploited an evolutionary transition that led to the loss of larval trichomes in *D. sechellia*, a species closely related to *D. melanogaster* (Stern and Frankel, 2013). *D. sechellia* adults, like *D. melanogaster* adults, are completely covered with trichomes (data not shown), and *D. sechellia* males display an A4 and A5 trichome pattern identical to that of *D. melanogaster* (Figure 5B). In contrast, *D. sechellia* first-instar larvae, unlike *D. melanogaster* larvae, differentiate naked cuticle in dorso-lateral quaternary cells, because of a restricted loss of *svb* expression in embryos (Stern and Frankel, 2013; Frankel et al., 2010; McGregor et al., 2007). We have previously shown that the appearance of naked cuticle in the larva of *D. sechellia* resulted from loss of embryonic activity in five *svb* enhancers and that in the *D. sechellia E6* enhancer, this loss of activity was caused by single nucleotide changes in transcription factor binding sites (Frankel et al., 2011; Preger-Ben Noon et al., 2016). We therefore reasoned that analyzing the activity of *D. sechellia svb* enhancers may reveal site pleiotropy.

First, we tested whether pupal *svb* expression is conserved in *D. sechellia*. We generated a *D. sechellia* BAC, named *D. sechellia svb*BAC-GFP, with the same genomic boundaries as the *D. melanogaster svb*BAC-GFP and a nuclear GFP inserted in the same site as the *D. melanogaster svb*BAC-GFP (Figure S6A). The *D. sechellia svb*BAC-GFP recapitulated the embryonic expression pattern of *D. sechellia svb*, and no expression was detected in dorso-lateral quaternary cells of the epidermis (compare Figures S6B and S1B). In addition, the *D. sechellia svb*BAC-GFP drove GFP expression throughout the dorsal and ventral pupal epidermis, just like the *D. melanogaster svb*BAC-GFP (Figure S6C). Therefore, it is likely that some *D. sechellia svb* enhancers that lost embryonic expression still drive expression in pupa. To explore this issue further, we examined the embryonic and pupal functions of two *svb* enhancers in more detail.

We first compared the activity of *Z1.3* and *E6* from *D. melanogaster* and *D. sechellia* in embryos. These two enhancers (Figure 6A) drive partially overlapping expression patterns in the dorso-lateral epidermis of *D. melanogaster* stage 15 embryos (Figures 6B and 6D; Frankel et al., 2011). On the other hand, the orthologous sequences from *D. sechellia* drive greatly reduced (*secZ1.3*) or absent (*secE6*) embryonic expression (Figures 6C and 6E). We next compared the activity of *Z1.3* and *E6* from *D. melanogaster* and *D. sechellia* in pupal stages. The *melZ1.3* enhancer recapitulated the full *Z* expression pattern in pupae (Figure 3), including expression in the wings (Figure 6F), legs (Figure 6H), and abdomen (Figure 6J). Despite

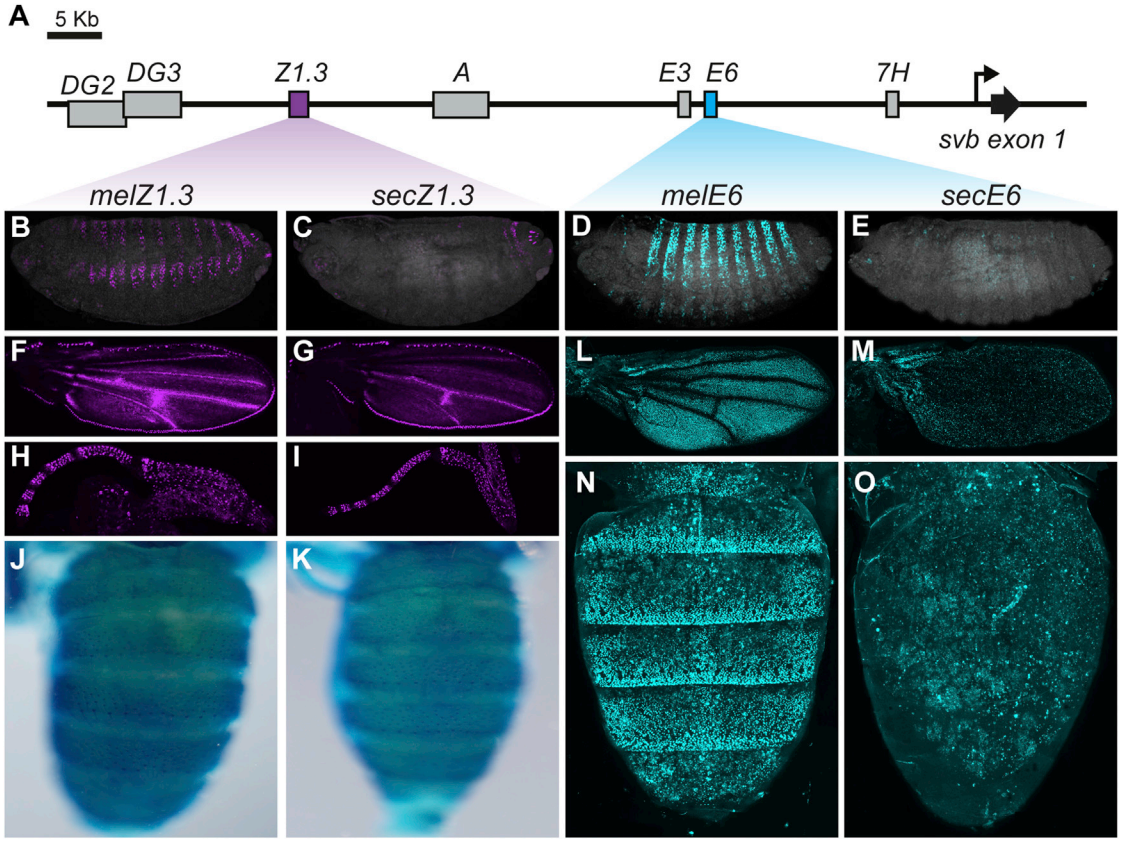

Figure 6. The *D. sechellia Z1.3* Enhancer Drives Conserved Pupal Expression, Whereas the *D. sechellia E6* Enhancer Lost Its Pupal Functions

(A) Schematic representation of the *svb* locus, indicating embryonic enhancers (light gray boxes). The *Z1.3* and *E6* enhancers are highlighted in magenta and cyan, respectively. The first exon of *svb* is indicated in black.

(B–E) Expression driven by *D. melanogaster Z1.3* (B; *melZ1.3*), *D. sechellia Z1.3* (C; *secZ1.3*), *D. melanogaster E6* (D; *melE6*) and *D. sechellia E6* (E; *secE6*) in *D. melanogaster* stage 15 embryos.

(F–K) Expression of *melZ1.3* (F, H, and J) and *secZ1.3* (G, I, and K) in *D. melanogaster* pupal wings (F and G; 36 hr AFP), legs (H and I; 36 hr APF), and dorsal abdominal epidermis of the pupa (J and K; 74 hr AFP).

(L–O) Expression driven by *melE6* (L and N) and *secE6* (M and O) in pupal wings (L and M; 74 hr APF) and dorsal abdomen (N and O; 84 hr APF).

the loss of its embryonic activity, the *secZ1.3* enhancer drove expression in all tissues where *melZ1.3* is active (Figures 6G, 6I, and 6K). Therefore, the genetic changes that led to the loss of *Z1.3* expression in *D. sechellia* embryos did not inactivate *Z1.3* function in pupae. Conversely, although *melE6* drove strong expression in the wing and dorsal abdomen of the pupa (Figures 6L and 6N), *secE6* did not drive expression in these pupal tissues (Figures 6M and 6O). Thus, it is possible that the changes in transcription factor binding sites that inactivated *secE6* in the embryo also affected pupal expression.

Spatially Separated Regulatory Information Generates the Various Expression Patterns of *Z1.3*

The finding that *secZ1.3* retained its pupal function while having lost most of its embryonic activity raised the possibility that the regulatory information encoding the embryonic and pupal patterns is spatially separated. To test this hypothesis, we dissected *melZ1.3* into smaller fragments and tested their ability to drive expression in embryo and pupa (Figure S7). We found that embryonic expression is encoded in a 300 bp fragment named *melZ0.3* (Figure S7), while pupal expression is encoded by the adjacent fragment *melZ1.3R* (Figure S7). In agreement with the results for *secZ1.3*, we found that *secZ1.3R* drove expression in pupal epidermis (data not shown). Taken together these results indicate that the *Z* enhancer drives embryonic and pupal expression patterns through adjacent sequences and suggest that the two patterns are generated with different transcription factor binding sites.

Site Pleiotropy: The Same Transcription Factor Binding Sites within *E6* Are Used in Both Embryo and Pupa

The loss of *secE6* expression in embryos and pupae suggested the possibility that the same transcription factor binding sites within *E6* are used in both developmental contexts. We have previously shown that *melE6* contains multiple transcription factor binding sites for the transcriptional activators Arrowhead (Awh) and Pannier (Pnr) (Figure 7A; Preger-Ben Noon et al., 2016). Most of these binding sites are conserved in *E6* of *D. simulans* (*simE6*), a species closely related to *D. melanogaster* (Figure 7A; Preger-Ben Noon et al., 2016). In contrast, the *secE6* enhancer

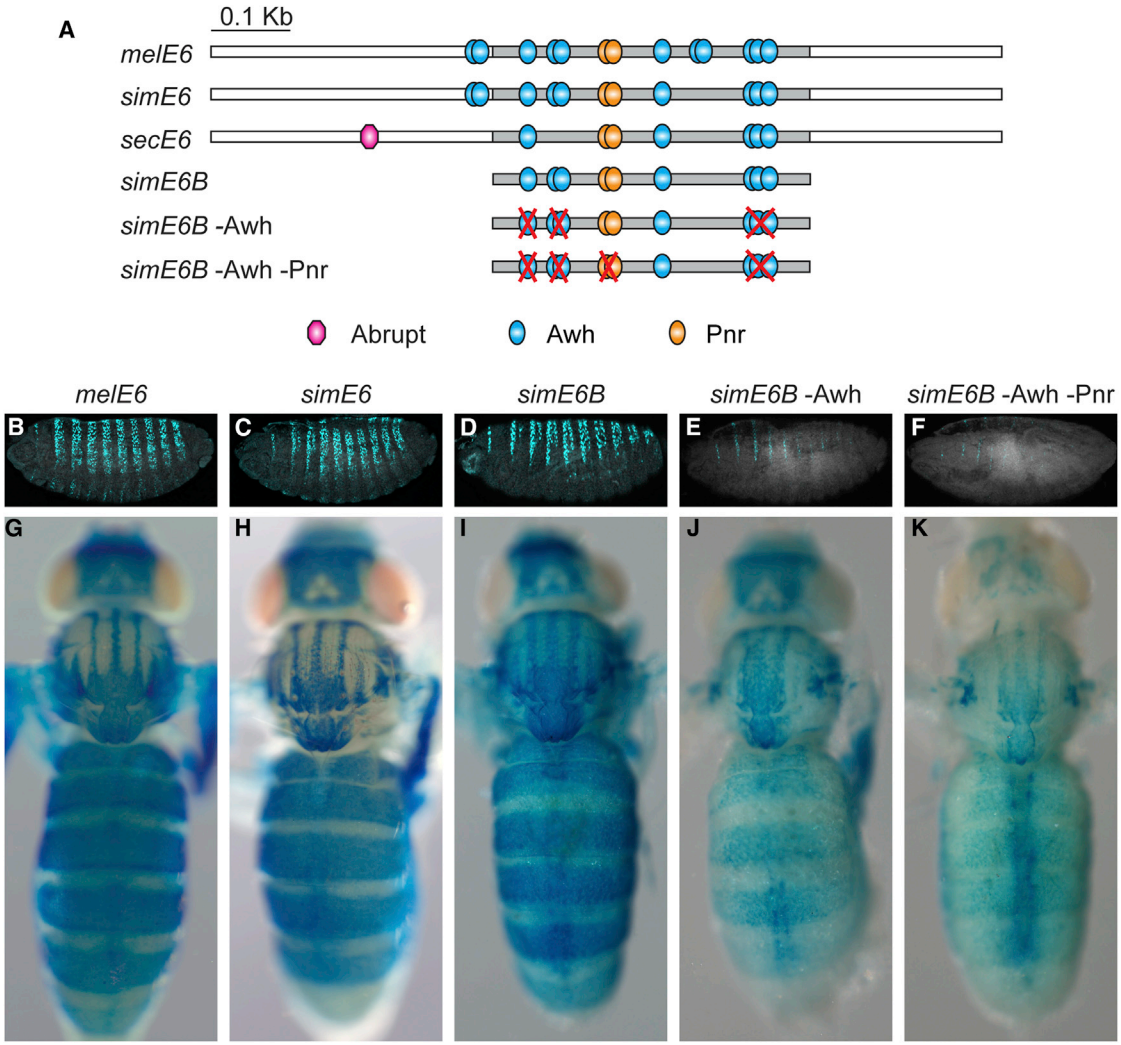

Figure 7. Reuse of Transcription Factor Binding Sites in the Pleiotropic Enhancer *E6*

(A) Scheme of *E6* from *D. melanogaster* (*melE6*), *D. simulans* (*simE6*), *D. sechellia* (*secE6*), and the wild-type and mutated *simE6B* constructs used in this study. Gray boxes indicate the location of the minimal enhancer *E6B*, within *E6*. Cyan and orange ovals represent binding sites for the activators Awh and Pnr, respectively. The binding site for the repressor Abrupt in *secE6* is represented by a magenta octagon. Red crosses indicate mutated activator binding sites.
(B–F) Expression driven by *melE6* (B), *simE6* (C), *D. simulans E6B* (D; *simE6B*) and *simE6B* mutants (E and F) in *D. melanogaster* stage 15 embryos.
(G–K) Expression driven by *melE6* (G), *simE6* (H), *simE6B* (I), and *simE6B* mutants (J and K) in *D. melanogaster* pupa (74 hr APF).

lost four Awh sites and gained a transcription factor binding site for the strong repressor Abrupt (Ab), causing the complete loss of its embryonic function (Figures 6E and 7A; Preger-Ben Noon et al., 2016). We therefore examined the contribution of individual classes of transcription factor binding sites to the functions of *E6*, using fly lines carrying mutated versions of the minimal enhancer, *E6B* (Figure 7A). We had previously shown that *melE6B* and *simE6B* recapitulate the embryonic expression pattern of the full *E6* (compare Figures 7C and 7D) and that mutation of Awh and Pnr sites within *simE6B* dramatically reduce its embryonic expression (Figures 7A, 7E, and 7F; Preger-Ben Noon et al., 2016). Given the equivalence of *melE6B* and *simE6B* and because we already had generated *simE6B* mutant lines, we decided to work with *simE6B* instead of *melE6B*. Analysis of *simE6B* expression revealed that, like the full-length *simE6* and *melE6,* this minimal enhancer also drives pupal expression (Figures 7G–7I). Remarkably, disruption of the Awh sites from *simE6B* eliminated most pupal abdominal expression (Figure 7J). Further mutation of Awh sites and two Pnr sites led to an even stronger reduction in pupal expression (Figure 7K). We have previously demonstrated that many Awh sites in *simE6B* are required for robust embryonic expression (Preger-Ben Noon et al., 2016). However, we cannot rule out that in the pupa, only a subset of these sites are required for proper enhancer function. Altogether, and in contrast to our observations for the *Z* enhancer, these experiments demonstrate that transcription factor binding sites within *E6* are "reused" at multiple developmental stages.

DISCUSSION

The *svb* gene encodes a master transcription factor that determines the fate of epidermal cells in *Drosophila melanogaster* (Delon et al., 2003). It has been known for some time that the embryonic activity of SVB is necessary to pattern the first-instar larva cuticle (Payre et al., 1999). We found that *svb* is expressed in several structures of third-instar larvae that have an ectodermal origin (foregut, CNS, imaginal discs, and epidermis). Furthermore, guided by previous research (Chanut-Delalande et al., 2014; Delon et al., 2003), we found that *svb* is expressed throughout the pupal epidermis and that this expression is required for the development of most adult trichomes. In summary, we have shown that *svb* is a pleiotropic gene.

The seven *svb* enhancers that drive expression in the embryo also generate expression in third-instar larvae and pupae. Thus, the seven enhancers of *svb* are pleiotropic enhancers. Similarly, small DNA fragments of other *Drosophila* genes can drive expression in various tissues (Monteiro and Podlaha, 2009). Recently, chromatin conformation assays showed that the same genomic regions are active in the regulation of gene expression in both developing limb and developing genitalia of mouse (Lonfat et al., 2014). These data strongly suggested that single enhancers might be used in multiple developmental contexts (Lonfat et al., 2014). Later studies reported that the HLEB enhancer of the *Tbx4* gene functions during both limb and genitalia formation with a similar epigenetic landscape, corroborating the idea that the same regulatory element can be active in two dissimilar contexts (Infante et al., 2015). Altogether, our data and previous reports (Schep et al., 2016; Lonfat et al., 2014; Infante et al., 2015; Monteiro and Podlaha, 2009) suggest that enhancer pleiotropy might be a common feature of *cis*-regulatory regions. A possible explanation for the pleiotropic role of enhancers is that these regions of the genome are structurally or topologically special, and that their qualities facilitate the interaction with basal promoters. This idea is supported by the fact that there is conservation in the positioning of enhancers in distant lineages (Frankel et al., 2012; Cande et al., 2009). Alternatively, it can be hypothesized that new expression patterns are easier to evolve within pre-existing epigenetic landscapes.

There are two fundamentally distinct models by which pleiotropic enhancers could encode different expression patterns. First, the same transcription factor binding sites could be used to drive expression in different contexts (i.e., there is site pleiotropy) or, second, distinct transcription factor binding sites within the same enhancer region could drive different patterns. We studied two pleiotropic *svb* enhancers in detail and in one case we detected site pleiotropy. We uncovered that Awh and Pnr binding sites, which activate enhancer *E6* in the embryo, are also needed to activate *E6* in the pupa. Similarly, it has been shown that Abd-B and STAT binding sites are required for the function of a *Poxn* enhancer in two developmental contexts (Glassford et al., 2015). In contrast, in the *svb Z1.3* enhancer, we found that transcription factor binding sites that function in the embryo and pupa act independently. This type of architecture might explain how the *Tbx4* enhancer lost its hindlimb function in snakes without losing its activity in genitalia (Infante et al., 2015).

Enhancer function is often schematized as strongly modular, with a single DNA fragment driving a single expression pattern (for examples, see Smith and Shilatifard, 2014; Krijger and de Laat, 2016; Gilbert, 2010). This schematization, though generally made to illustrate a concept, is misleading. Our results suggest that enhancer pleiotropy might be a common phenomenon and that transcription factor binding sites can be "reused" during development. These observations challenge the notion that enhancers are active in a single developmental context. In addition, the "reuse" of transcription factor binding sites may impose constraints on how enhancers can evolve new functions.

We observed extensive redundancy of *svb* enhancer activity in pupal stages. This redundancy far exceeds the redundancy we had characterized previously for the embryonic expression pattern, which is required for phenotypic robustness (Preger-Ben Noon et al., 2016; Frankel et al., 2010). In fact, we observed that deleting individual enhancers has contrasting outcomes in embryos and pupae. Whereas in embryos the loss of one enhancer diminishes gene expression, in pupae the lack of a single enhancer generates a slight increase in gene expression. This counterintuitive result could be explained with a model of enhancer-promoter competition (Bothma et al., 2015; Long et al., 2016), in which an enhancer impedes the interaction of other enhancers with the promoter. In addition, we observed that flies carrying only three of the total seven *svb* enhancers still produce largely normal adult trichome patterns, even when pupae are grown under stressful conditions. In summary, the function of *svb cis*-regulatory region in pupa appears to result in strong robustness of the adult trichome pattern.

We have shown that *svb* enhancers are pleiotropic and that their expression is highly redundant. Indeed, in *D. sechellia* these enhancers drive enough pupal *svb* expression through stage-specific transcription factor binding sites that the embryonic expression pattern was free to evolve without altering the adult expression pattern. However, it is also possible to imagine a scenario with less redundancy and in which site pleiotropy is a significant factor (as in the case of enhancer *E6*), which would constrain the evolution of expression patterns. At present, it is unclear how many enhancers in the genome are pleiotropic and whether site pleiotropy is pervasive. Further studies should help determine the extent of pleiotropy, clarifying its potential role in evolution.

EXPERIMENTAL PROCEDURES

Genetic Constructs and Transgenesis

P[acman] CH321-64E24 (https://bacpacresources.org) contains a 91,307 bp insert that includes the *cis*-regulatory region, the first exon, and part of the first intron of *shavenbaby* (https://www.ncbi.nlm.nih.gov/clone/33521512). We used BAC recombineering (Wang et al., 2009) to insert a GFP-nuclear localization signal (NLS) or a DsRed-NLS in the initiation codon of *svb* to generate *svb*BAC-GFP and *svb*BAC-DsRed and to delete specific enhancers in the context of *svb*BAC-GFP. All primers and constructs that were used for BAC recombineering are summarized in Table S1.

The *D. sechellia svb* gene, including the *cis*-regulatory region, the first exon, and part of the first intron (droSec1: super_4:1,797,878-1,880,229) was subcloned from the BAC DSE1-007L13 (RIKEN BioResource Center DNA Bank) into P[acman]. Subsequently, BAC recombineering was used to insert a GFP-NLS in the initiation codon of *svb* to generate *sec-svb*-BAC-GFP.

The GFP-NLS in pS3AG (a gift from Thomas Williams, Addgene plasmid #31171) was replaced with a DsRed-NLS to generate pS3AR. The DsRed-NLS was released from pRed H-Stinger with enzymes XhoI and SpeI. GFP-NLS was removed from pS3AG by cutting with enzymes XhoI and SpeI. The pS3AG backbone (without GFP-NLS) was then ligated to the DsRed-NLS. All other transgenes generated in this study were constructed by GenScript (summarized in Table S2). These constructs were integrated into the fly genome through attP/attB recombination (Rainbow Transgenic Flies).

Fly Strains

Enhancer-reporter lines are summarized in Table S2. To generate *Df(X)svb*^{106}, pBacPtp4E[f02952] and pBac[f06356] were recombined onto the same X chromosome, and a homozygous stock was generated. This stock was crossed to a line containing a hs::flipase and larvae were heat-shocked at 37°C for 1 hr each day during larval development. After crossing these adults to *white* flies, we selected adults that had lost one copy of the *white*$^{+}$ transgene (originating on one of the pBac transgenes), which is expected if the two FRT sites recombined to generate a deletion. The deletion was confirmed by PCR, with primers located outside the deletion (5′-CGTACCGCCTGTTTGCCATA-′3 and 5′-TCCAGACGGATTTTATGGCC-′3), which amplified the expected 7.3 kb fragment containing a pBac transposon. We then generated a stock homozygous for the deletion. *Df(X)svb*^{108} was described previously (Frankel et al., 2010). *D. sechellia* 14021-0248.28 was obtained from the *Drosophila* Species Stock Center at the University of California.

We generated large clonal territories of *svb*$^{-}$ tissue by using the Minute technique (Morata and Ripoll, 1975). With this technique, clones that contain two wild-type alleles of *Minute*$^{+}$ over-proliferate relative to neighboring cells that are heterozygous for a *Minute* null mutation. To mark *svb*$^{-}$ tissue, we recombined three visible markers (y^{1}, w^{1}, and f^{36a}) onto a chromosome together with a null mutation for *svb* (*svb*^{1}), to generate y^{1} w^{1} *svb*^{1} f^{36a}. We then crossed this strain to flies carrying a dominant Minute allele on the X chromosome. We exposed larvae carrying the genotype y^{1} w^{1} *svb*^{1} f^{36a} / M to x-Rays (1,000 rad) 24–72 hr after egg laying. We screened females for clones homozygous for *svb*^{1} by searching for cuticle containing bristles that were both yellow and forked. We compared trichome patterns in these clones with trichome patterns on flies homozygous for the f^{36a} allele.

X-Gal Staining

Third-instar larvae were dissected in PBS and fixed in PBS with 4% formaldehyde for 10 min. Staged pupae were removed from the pupal case and then fixed in PBS with 4% formaldehyde for 15 min. After washing in PBT (1× PBS + 0.1% Triton X-100), samples were incubated with X-Gal solution (5 mM $K_4[Fe^{+2}(CN)_6]$, 5 mM $K_3[Fe^{+2}(CN)_6]$, 1 mg/ml X-Gal in PBS and Triton 0.1% [PBT]) at 37°C for 1 hr. The samples were mounted and imaged with bright-field microscopy.

Immunofluorescence

Stage 15 embryos were collected, fixed, and stained using standard protocols with chicken anti-GFP (1:300; Aves Labs), rabbit anti-RFP (1:150; MBL), mouse anti-βGal (1:500; Promega), anti-chicken Alexa Fluor 488 (1:250; Thermo Fisher Scientific), anti-rabbit Alexa Fluor 647 (1:150; Thermo Fisher Scientific) and anti-mouse Alexa Fluor 546 (1:400; Thermo Fisher Scientific). Pupal tissues were dissected, fixed, and stained with mouse anti-βGal and anti-mouse Alexa Fluor 546 as described (Halachmi et al., 2012).

Microscopy and Image Analysis

Embryos were prepared using standard protocols and immunostained with the antibodies described above. Pupae of the desired stages were removed from the pupal case and placed in a microscope slide for imaging. To analyze the effect of enhancer deletions in *svb*BACs we measured GFP and DsRed levels in embryos and pupae carrying *svb*BAC-GFP (wild-type and deletions) and *svb*BAC-DsRed (wild-type). GFP and DsRed signals were measured sequentially over a z stack in a confocal microscope. Images were analyzed using ImageJ software (http://rsb.info.nih.gov/ij/). First, background was subtracted using a 50-pixel rolling-ball radius in each slice of the confocal z stack. Then, we calculated the Sum projection of the z stacks for each channel in order to compare GFP versus DsRed levels. Max projections were obtained in order to analyze GFP levels between abdominal segments A4 and A5. For embryos, we applied the segmentation masks using the Sum projection of the DsRed channel with the ImageJ autothreshold tool ("IJ_IsoData dark"). For pupal abdomens, segmentation masks were applied with Ilastik 1.2.0 software (http://ilastik.org) to Sum projections of the GFP channel (GFP versus DsRed levels in A4) and Max projections (GFP levels in A4 and A5). We measured the fluorescence mean intensities of each nucleus with the "Analyze particles" tool in ImageJ. Then, we calculated the average of the fluorescence mean intensity of all segmented nuclei. Last, we calculated the ratio GFP/DsRed in each nucleus and calculated the average ratio for all segmented nuclei.

Cuticle Preparation

Adults were collected and frozen until used. Adult cuticles were dissected in PBS and mounted in a microscope slide with a drop of 1:1 Hoyer's:lactic acid mixture. After overnight drying, the cuticles of adults were imaged with bright-field microscopy. The images were processed using Adobe Photoshop.

SUPPLEMENTAL INFORMATION

Supplemental Information includes seven figures and two tables and can be found with this article online at https://doi.org/10.1016/j.celrep.2018.02.073.

ACKNOWLEDGMENTS

We would like to thank the two anonymous reviewers for their helpful comments on the manuscript. We thank François Payre for providing the f^{36a}/FM6 stock. We thank Xiaorong Zhang of the Janelia Molecular Biology Shared Resource for help with the *sec-svb*-BAC-GFP recombineering and the Janelia Fly core facility for help with fly work. We thank the Bioimaging Core Facility at the Technion Rappaport Faculty of Medicine for help with imaging. E.P.-B.N. is grateful for the generous hospitality of Adi Salzberg and her lab members. E.P.-B.N. was supported by postdoctoral fellowships from the Human Frontier Science Program (LT000528/2011). This work was supported in part by Fundación Bunge y Born and Agencia Nacional de Promoción Científica y Tecnológica (PICT 2013-2138) grants to N.F.

AUTHOR CONTRIBUTIONS

E.P.-B.N., G.S., D.L.S., and N.F. conceived experiments. E.P.-B.N., G.S., D.L.S., D.M.O., A.L., and N.F. performed experiments and analyzed data with technical help from J.S. E.P.-B.N. and N.F. wrote the manuscript with contributions from G.S. and D.L.S. E.P.-B.N. and G.S. contributed equally to this work and are listed in alphabetical order as authors.

DECLARATION OF INTERESTS

The authors declare no competing interests.

Received: September 21, 2017
Revised: January 31, 2018
Accepted: February 19, 2018
Published: March 13, 2018

REFERENCES

Arif, S., Kittelmann, S., and McGregor, A.P. (2015). From shavenbaby to the naked valley: trichome formation as a model for evolutionary developmental biology. Evol. Dev. *17*, 120–126.

Bothma, J.P., Garcia, H.G., Ng, S., Perry, M.W., Gregor, T., and Levine, M. (2015). Enhancer additivity and non-additivity are determined by enhancer strength in the *Drosophila* embryo. eLife *4*, 4.

Cande, J., Goltsev, Y., and Levine, M.S. (2009). Conservation of enhancer location in divergent insects. Proc. Natl. Acad. Sci. U S A *106*, 14414–14419.

Carroll, S.B. (2008). Evo-devo and an expanding evolutionary synthesis: a genetic theory of morphological evolution. Cell *134*, 25–36.

Chanut-Delalande, H., Hashimoto, Y., Pelissier-Monier, A., Spokony, R., Dib, A., Kondo, T., Bohère, J., Niimi, K., Latapie, Y., Inagaki, S., et al. (2014). Pri peptides are mediators of ecdysone for the temporal control of development. Nat. Cell Biol. *16*, 1035–1044.

Crocker, J., Abe, N., Rinaldi, L., McGregor, A.P., Frankel, N., Wang, S., Alsawadi, A., Valenti, P., Plaza, S., Payre, F., et al. (2015). Low affinity binding site clusters confer hox specificity and regulatory robustness. Cell *160*, 191–203.

Davidson, E.H. (2010). The regulatory genome: gene regulatory networks. In Development and Evolution (Elsevier Science).

Delon, I., Chanut-Delalande, H., and Payre, F. (2003). The Ovo/Shavenbaby transcription factor specifies actin remodelling during epidermal differentiation in *Drosophila*. Mech. Dev. *120*, 747–758.

Frankel, N. (2012). Multiple layers of complexity in cis-regulatory regions of developmental genes. Dev. Dyn. *241*, 1857–1866.

Frankel, N., Davis, G.K., Vargas, D., Wang, S., Payre, F., and Stern, D.L. (2010). Phenotypic robustness conferred by apparently redundant transcriptional enhancers. Nature *466*, 490–493.

Frankel, N., Erezyilmaz, D.F., McGregor, A.P., Wang, S., Payre, F., and Stern, D.L. (2011). Morphological evolution caused by many subtle-effect substitutions in regulatory DNA. Nature *474*, 598–603.

Frankel, N., Wang, S., and Stern, D.L. (2012). Conserved regulatory architecture underlies parallel genetic changes and convergent phenotypic evolution. Proc. Natl. Acad. Sci. U S A *109*, 20975–20979.

Gilbert, S.F. (2010). Developmental Biology (Sinauer Associates).

Glassford, W.J., Johnson, W.C., Dall, N.R., Smith, S.J., Liu, Y., Boll, W., Noll, M., and Rebeiz, M. (2015). Co-option of an ancestral Hox-regulated network underlies a recently evolved morphological novelty. Dev. Cell *34*, 520–531.

Halachmi, N., Nachman, A., and Salzberg, A. (2012). Visualization of proprioceptors in *Drosophila* larvae and pupae. J. Vis. Exp. (*64*), e3846.

Infante, C.R., Mihala, A.G., Park, S., Wang, J.S., Johnson, K.K., Lauderdale, J.D., and Menke, D.B. (2015). Shared enhancer activity in the limbs and phallus and functional divergence of a limb-genital cis-regulatory element in snakes. Dev. Cell *35*, 107–119.

Kim, A.R., Martinez, C., Ionides, J., Ramos, A.F., Ludwig, M.Z., Ogawa, N., Sharp, D.H., and Reinitz, J. (2013). Rearrangements of 2.5 kilobases of noncoding DNA from the *Drosophila* even-skipped locus define predictive rules of genomic cis-regulatory logic. PLoS Genet. *9*, e1003243.

Krijger, P.H., and de Laat, W. (2016). Regulation of disease-associated gene expression in the 3D genome. Nat. Rev. Mol. Cell Biol. *17*, 771–782.

Lonfat, N., Montavon, T., Darbellay, F., Gitto, S., and Duboule, D. (2014). Convergent evolution of complex regulatory landscapes and pleiotropy at Hox loci. Science *346*, 1004–1006.

Long, H.K., Prescott, S.L., and Wysocka, J. (2016). Ever-changing landscapes: transcriptional enhancers in development and evolution. Cell *167*, 1170–1187.

McGregor, A.P., Orgogozo, V., Delon, I., Zanet, J., Srinivasan, D.G., Payre, F., and Stern, D.L. (2007). Morphological evolution through multiple cis-regulatory mutations at a single gene. Nature *448*, 587–590.

Montavon, T., Soshnikova, N., Mascrez, B., Joye, E., Thevenet, L., Splinter, E., de Laat, W., Spitz, F., and Duboule, D. (2011). A regulatory archipelago controls Hox genes transcription in digits. Cell *147*, 1132–1145.

Monteiro, A., and Podlaha, O. (2009). Wings, horns, and butterfly eyespots: how do complex traits evolve? PLoS Biol. *7*, e37.

Morata, G., and Ripoll, P. (1975). Minutes: mutants of Drosophila autonomously affecting cell division rate. Dev. Biol. *42*, 211–221.

Paaby, A.B., and Rockman, M.V. (2013). The many faces of pleiotropy. Trends Genet. *29*, 66–73.

Payre, F., Vincent, A., and Carreno, S. (1999). ovo/svb integrates Wingless and DER pathways to control epidermis differentiation. Nature *400*, 271–275.

Preger-Ben Noon, E., Davis, F.P., and Stern, D.L. (2016). Evolved repression overcomes enhancer robustness. Dev. Cell *39*, 572–584.

Pueyo, J.I., and Couso, J.P. (2011). Tarsal-less peptides control Notch signalling through the Shavenbaby transcription factor. Dev. Biol. *355*, 183–193.

Schep, R., Necsulea, A., Rodríguez-Carballo, E., Guerreiro, I., Andrey, G., Nguyen Huynh, T.H., Marcet, V., Zákány, J., Duboule, D., and Beccari, L. (2016). Control of Hoxd gene transcription in the mammary bud by hijacking a preexisting regulatory landscape. Proc. Natl. Acad. Sci. U S A *113*, E7720–E7729.

Smith, E., and Shilatifard, A. (2014). Enhancer biology and enhanceropathies. Nat. Struct. Mol. Biol. *21*, 210–219.

Stern, D.L. (2000). Evolutionary developmental biology and the problem of variation. Evolution *54*, 1079–1091.

Stern, D.L., and Frankel, N. (2013). The structure and evolution of cis-regulatory regions: the shavenbaby story. Philos. Trans. R. Soc. Lond. B Biol. Sci. *368*, 20130028.

Wang, S., Zhao, Y., Leiby, M., and Zhu, J. (2009). A new positive/negative selection scheme for precise BAC recombineering. Mol. Biotechnol. *42*, 110–116.

Williamson, I., Lettice, L.A., Hill, R.E., and Bickmore, W.A. (2016). Shh and ZRS enhancer colocalisation is specific to the zone of polarising activity. Development *143*, 2994–3001.

Wittkopp, P.J., and Kalay, G. (2011). Cis-regulatory elements: molecular mechanisms and evolutionary processes underlying divergence. Nat. Rev. Genet. *13*, 59–69.

Zeitlinger, J., Zinzen, R.P., Stark, A., Kellis, M., Zhang, H., Young, R.A., and Levine, M. (2007). Whole-genome ChIP-chip analysis of Dorsal, Twist, and Snail suggests integration of diverse patterning processes in the *Drosophila* embryo. Genes Dev. *21*, 385–390.